Solution processed polymer light-emitting diodes with single layer graphene anode

Article *in* Proceedings of SPIE - The International Society for Optical Engineering · September 2012

DOI: 10.1117/12.928821

7 authors, including:

Changhee Lee
Seoul National University
330 PUBLICATIONS **4,650** CITATIONS

Organic Electronics 14 (2013) 2324–2330

Contents lists available at SciVerse ScienceDirect

Organic Electronics

journal homepage: www.elsevier.com/locate/orgel

High-performance polymer light emitting diodes with interface-engineered graphene anodes

Jaeheung Ha [a,1], Subeom Park [b,1], Donghyun Kim [a], Jaechul Ryu [c], Changhee Lee [a], Byung Hee Hong [b,c,*], Yongtaek Hong [a,*]

[a] Department of Electrical and Computer Engineering, Seoul National University, Seoul 151-757, Republic of Korea
[b] Department of Chemistry, Seoul National University, Seoul 151-757, Republic of Korea
[c] SKKU Advanced Institute of Nanotechnology (SAINT), Center for Human Interface Nano Technology (HINT), Sungkyunkwan University, Suwon 440-746, Republic of Korea

ARTICLE INFO

Article history:
Received 10 April 2013
Received in revised form 14 May 2013
Accepted 19 May 2013
Available online 7 June 2013

Keywords:
Polymer light emitting diodes (PLEDs)
Graphene
Transfer length method (TLM)
Work function
Chemical vapor deposition (CVD)

ABSTRACT

Recently, graphene-based organic light emitting diodes (OLEDs) were successfully demonstrated using graphene as anodes. However, the graphene electrodes have not been utilized for polymer light emitting diodes (PLEDs) yet, although the simpler device structure and the solution-based fabrication process of PLEDs are expected to be more advantageous in terms of time and cost. Here we demonstrate high-performance polymer light emitting diodes (PLEDs) with simple two-layer structures using interface-engineered single-layer graphene films as anodes. The single-layer graphene synthesized by chemical vapor deposition methods was transferred onto a glass substrate utilizing an elastic stamp, and its work function was engineered by varying the duration and the power of ultraviolet ozone (UVO) treatment. Thus, we were able to optimize the contact between silver electrodes and the graphene anodes, leading to the considerable enhancement of light-emitting performance.

1. Introduction

Since the first isolation of graphene in 2004 [1], graphene-based transparent electrodes have received remarkable attentions in the photonic and optoelectronic applications [2] including organic light emitting diodes (OLEDs) [3–6], photovoltaic cells [7], light emitting electrochemical cells (LECs) [8,9], and touch sensors [10]. Although indium tin oxide (ITO) is being mainly used as transparent electrode materials in various display and photovoltaic applications, its brittleness, high fabrication cost, and poor surface property have limited the actual performance of optoelectronic devices [11]. Moreover, the diffusion of the indium into the organic layer causes OLED luminance degradation due to luminescence quenching [12]. On the contrary, the graphene electrode is expected to show not only high conductivity and outstanding transmittance but also ultrahigh flexibility, chemical inertness, and smooth interface with controllable work functions, which made it one of the most promising candidates that can replace ITO in the future [10]. In practice, several papers have already reported the use of graphene electrodes for OLED applications [3–6]. However, most of them show rather low current and power efficiencies unless additional hole injection materials or complicated multi-layered structures are adopted. On the other hand, the use of graphene electrodes for polymer light emitting diodes (PLEDs) with simple bi-layer structures has not been reported yet, although PLEDs are expected to be more advantageous than OLEDs in terms of processibility, flexibility, fabrication and materials costs [13].

* Corresponding authors. Address: Department of Chemistry, Seoul National University, Seoul 151-757, Republic of Korea. Tel.: +82 2 880 6569 (B.H. Hong), +82 2 880 9567 (Y. Hong).
E-mail addresses: byunghee@snu.ac.kr (B.H. Hong), yongtaek@snu.ac.kr (Y. Hong).
[1] These authors contributed equally to this work.

1566-1199/$ - see front matter © 2013 Elsevier B.V. All rights reserved.
http://dx.doi.org/10.1016/j.orgel.2013.05.033

In most cases, multi-layer graphene electrodes are being used rather than single-layer graphene to achieve higher conductivity [3–6]. However, the sheet resistance of graphene does not critically limit the optoelectronic performance in the case of bottom emission type active-matrix organic light emitting diodes (AMOLED) because the transparent electrodes are used only in a patterned manner just for individual pixels if the pixel can be emitted uniformly. Therefore, in this case, appropriate methods of patterning and work function engineering to achieve lower contact resistance between graphene electrodes and metal lines are more crucial than conductivity itself.

Thus, we demonstrate, for the first time, the fabrication of high-performance PLEDs using chemically modified single-layer graphene electrode as an anode to maximize the optoelectronic performance. Ultraviolet ozone (UVO) treatment was utilized to pattern and engineer the work function of the single-layer graphene films. The contact resistance between single-layer graphene films and several metal layers were also investigated.

2. Experiment and measurements

2.1. Preparation of graphene substrates

Monolayer graphene was synthesized by utilizing a chemical vapor deposition (CVD) process described in the literature [10]. The graphene film grown on the copper foil was covered by poly(methyl methacrylate) (PMMA) and floated on the surface an aqueous solution of 0.1 M ammonium persulphate ($(NH_2)_4S_2O_8$). After all the copper layers were etched away, submerging a clean PET film into the etchant and picking up the floating PMMA/graphene film to transfer it into DI water. The cleaning process was repeated 5 times. The graphene film with PMMA support was transferred to the glass. To measure Raman spectrum, the monolayer graphene film was transferred to the SiO_2/Si substrate. The sample was dried with blowing nitrogen gas immediately, and was baked for 8 h on the hot plate at 60 °C, followed by cleaning in acetone at room temperature for 30 min to remove the PMMA support layer. Finally, the sample was dried and baked as previously done.

2.2. Patterning of graphene films and preparation of the TLM measurements

Graphene film on a glass substrate was etched with the shadow mask by illuminating the UVO in the air. The etching time was 15 min. Then, the several metal such as Ag (99.99%, Materion Advanced Chemical, USA), Al (99.999%, CERAC, USA), Ti (99.995%, CERAC, USA) was deposited in the vacuum chamber under 5.0×10^{-6} torr with the deposition rate at 5.0 Å/s, 2.0 Å/s, and 1.0 Å/s, respectively.

2.3. Fabrication of PLEDs

For a reference device, the glass substrate with ITO patterns purchased from Free M Tech (Korea) was cleaned in a ultrasonic bath with acetone, isopropyl alcohol (IPA), and deionized water for 10 min each at room temperature, consecutively. Then, the substrate was dried in an oven for 1 h at 120 °C. For the PLEDs with single-layer graphene anodes, additional Ag electrodes were deposited under 5.0×10^{-6} torr in a vacuum chamber. The rate of deposition and the thickness of the Ag electrode is 5.0 Å/s and 1500 Å, respectively. To control the work function of anodes and to remove any organic contaminants, the substrate was treated by UVO for 5 min for the graphene PLEDs, and for 10 min for the ITO PLEDs. The power of UV lamp (Low Pressure Mercury Vopar Grid Lamp, Jelight) was 28 mW/cm^2. After the UVO treatment, the substrate was transferred to a globe box to minimize the concentration of H_2O and O_2 during device fabrication. PEDOT:PSS (Poly(3,4-ethylenedioxythiophene) poly(styrenesulfonate), CLEVIOS™ P VP Al 4083, Heraeus, Germany) was spun-coated at 2000 rpm for 60 s. Then, annealing process was followed at 120 °C for 10 min. SPG-01T (Merck, Germany) that is a green emitting polymer was spun-coated by using 0.8 wt% concentrations in toluene solvent at 2000 rpm for 60 s. The substrate was annealed at 90 °C for 60 min, and then, Ca (99.99%, Sigma-Aldrich) was deposited at 1.0 Å/s rate in a vacuum chamber under 5.0×10^{-6} torr. Without breaking vacuum, Al was deposited at 2.0 Å/s rate under 5.0×10^{-6} torr.

2.4. Measurements

The SEM images of device structures and the atomic force microscopy (AFM) images of graphene films were taken by a field emission scanning electron microscope (FE-SEM, Hitachi S-48000) and by a non-contact mode AFM system (XE-100, Park system), respectively. The work function was measured by photoemission yield spectroscopy (AC-2, Riken Keiki). The Raman spectrums were measured by a Raman spectrometer (Raman microsystem 2000, Renishaw). The thickness and the sheet resistance were measured by a surface profiler (Surfcorder ET3000i, Kosaka) and a four point probe measuring system (FPP-5000, Changmin, Korea), respectively. The resistance between adjacent electrodes for a transfer length method (TLM) and the patterning process optimization were measured by a semiconductor parameter analyzer (HP4145B, HP). Current (I) – Voltage (V) – Luminance (L) characteristics were measured by a digital multimeter (Keithley 2000, Keithley) and a source-measure unit (Keithley 236, Keithley) while sweeping voltages. The measured data were calibrated by a spectroradiometer (CS-1000A, Konica Minolta).

3. Results and discussion

Fig. 1a shows the fabrication process of our PLEDs. The thickness of PEDOT:PSS and SPG-01T layers are 24 and 70 nm, respectively. The thickness of Ca and Al electrodes are 30 and 150 nm, respectively. Schematic structure of the device with ITO (reference), and single-layer graphene anodes are shown in Fig. 1b and c, respectively. Corresponding cross-sectional SEM images are shown in Fig. 1d and e. Except for anode layer, device structures of both PLEDs are identical. The emission area was 1.6×1.4 mm^2.

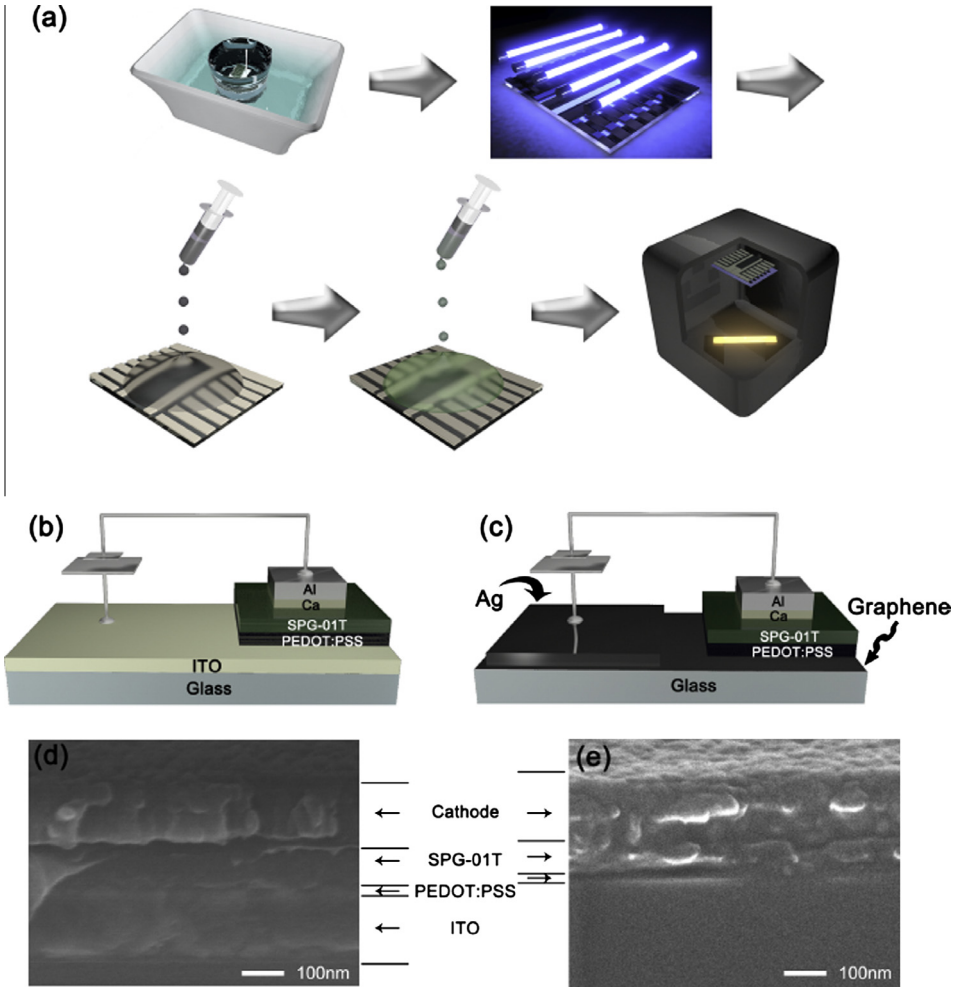

Fig. 1. Procedure and structure of PLEDs (a) fabrication procedure of PLEDs, (b) schematic image of PLEDs with ITO anode, (c) schematic image of PLEDs with graphene anode, (d) cross sectional SEM image of PLEDs with ITO anode and (e) cross sectional SEM image of PLEDs with graphene anode.

Two dimensional surface morphology of the graphene film on glass substrate is examined by using AFM as shown in Fig. 2a and Table 1. The graphene film on the glass substrate exhibits a smooth surface with peak-to-peak features 5.31 ± 0.15 nm and root mean square (RMS) roughness under 1 nm. To confirm single-layer film formation on glass substrates, the transferred graphene film was characterized by Raman spectroscopy and ultraviolet visible spectrophotometer. The Raman spectrums before and after UVO treatment are shown in Fig. 2b, and transmittance of the graphene film is shown in our previous report [14]. I_{2D}/I_G ratio and transmittance at 550 nm of the graphene film before UVO treatment are 4.521 and 97.5%, respectively. The results of the Raman spectrum and the transmittance are consistent with previously reported paper [15] and we confirm that graphene films used in this paper are single-layer.

Graphene films can be patterned by several methods, including photocatalytic patterning [16], scanning tunneling microscope lithography [17], anisotropic etching [18], oxidation [19], and plasma etching with chemically synthesized nanowires as an etch mask [20]. Although the conventional photolithography with O_2 plasma etching is an accurate patterning method, the patterned films typically have lots of contaminants originated from the photoresist residues and it requires complex processes [16]. In order to simplify the patterning process and to obtain high quality graphene films, we have patterned graphene film using UVO treatment with a shadow mask. The exposure time has been optimized by monitoring resistance (R) between adjacent patterned electrodes as shown in Fig. 3a. Fig. 3b shows that the resistance did not significantly change when the single-layer graphene films were exposed to UVO less than 5 min. Moreover, Raman spectra show that the graphene film holds the single layer property until 5 min of UVO treatment, which results are supported by the intensity ratio of 2D to G band (I_{2D}/I_G) (Fig. 2b). The I_{2D}/I_G ratio is varied from 4.521 to 1.616 and full-width half-maximum (FWHM) is increased from 25.92 to 46.72 cm^{-1} that are summarized in Table 2. The decrease of the height and broadening of the 2D bands is due to the oxygen containing groups including C═O, O—C═O, and C—O bonds on the graphene surface that are appeared while the graphene films are exposed to

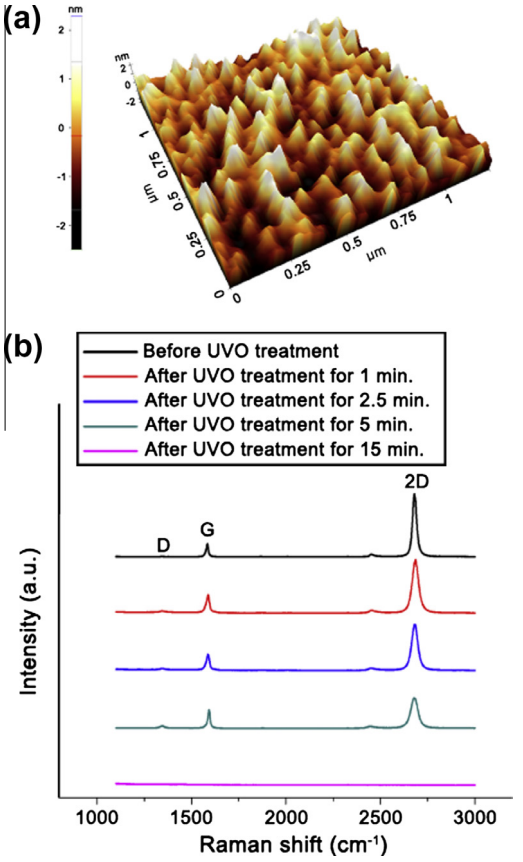

Fig. 2. (a) AFM image of single-layer graphene on the glass substrate and (b) Raman spectrum of single-layer graphene before and after UVO treatment.

UVO [21]. After about 15 min, Figs. 2b and 3b show that the resistance is infinite and the peaks in the Raman spectrum are disappeared. The single-layer graphene films were completely removed from the exposed area, and resultantly, electrically isolated graphene electrode patterns were formed. If the power of and the distance to the UV lamp in the system are optimized, the process time can be further reduced. However, in this study, for a proof of concept purpose, the 15-min process condition was used to pattern the single-layer graphene films.

One interesting observation during the UVO treatment of graphene is that the work function can be effectively engineered by inducing chemical changes on the graphene surface, when the exposure time is less than 5 min. It is well known that the work function of the anode is very important in improving the efficiency of hole injection to the hole injection layer (HIL) or hole transport layer (HTL) of OLEDs. In fact, the UVO treatment is also a well-known technology to control the work function of the conventional ITO anode. However, it has not been applied yet work function of the graphene films, although several groups used different methods including wet chemical doping [10,22], AlO_x overlayer coating [23], electric field effect [24], and functionalization by self-assembled single-layers [25].

Table 1
Surface roughness of grapheme film on the glass substrates.

Substrate	Peak to peak (nm)	Root mean square (nm)
Single-layer graphene on glass	5.31 ± 0.15	0.92 ± 0.03

The duration of UVO treatment needs to be well controlled because the work function of the graphene film sensitively changes with the exposure time. Fig. 3c and d shows the work functions of the single-layer graphene and ITO films before and after the UVO treatment, which were measured by photoemission yield spectroscopy. This result clearly shows that the work function of the graphene film increases with time of the UVO treatment. The work functions of the UVO treated graphene film for 2.5 min and 5 min change by 0.18 eV and 0.27 eV, respectively, with respect to non-treated graphene layer. The work function of the ITO anode moves by 0.42 eV after UVO treatment for 10 min. The results show that UVO treatment can be effectively used to control the work function of both ITO and single-layer graphene films.

In a typical AMOLED display, there are several additional metal lines that span vertically or horizontally to operate individual sub-pixels. In most cases, low-resistance materials such as aluminum or aluminum alloys are used to implement those lines in contact with the patterned transparent anode electrodes. If there is significant contact resistance between the metal line electrodes and each pixel anode, undesired voltage drop can be induced at the contact area, resulting in the degradation of display uniformity. Therefore, it must be considered that the contact resistance between graphene and metal electrodes needs to be minimized in order to adopt graphene as the materials of pixel anodes. Thus, we used the TLM [26] to investigate the contact resistance properties between the single-layer graphene and the metal lines. The schematic experiment method of the TLM and the device top view are visualized in Fig. 4a and b, respectively. L is the length of the contact electrode (500 μm), Z is the width of the contact electrode (1 mm), W is the width of the patterned graphene (1.4 mm), and d is the contact spacing length (from 150 to 450 μm with an interval of 50 μm).

The sheet resistance of the single-layer graphene film and its contact resistance with various metal electrodes can be extracted from the graph of a total resistance as a function of the spacing distance (Fig. 4c): R_T is total resistance, R_{sh} is sheet resistance, L_T is transfer length, and R_c is contact resistance. Several combinations of potential metal electrodes (Ag, Al, Ti/Ag, Ti/Al) that can be applied for the display panels were investigated. The thickness of Ag and Al was 1500 Å, and that of Ti was 200 Å, which were all measured by a surface profiler. Fig. 4d shows that the sheet resistance of graphene single-layer is 914.38 ± 9.41 (Ω/sq). The specific contact resistivity (ρ_c) can be calculated with Eq. (1) [27], and the value between graphene single-layer and Ag, Al, Ti/Ag, and Ti/Al metal electrodes is 4.96×10^{-6}, 3.16×10^{-4}, 7.51×10^{-6}, and 5.39×10^{-4} Ω-mm^2, respectively.

$$\rho_c = (L_T)^2 \times R_{sh} \quad (1)$$

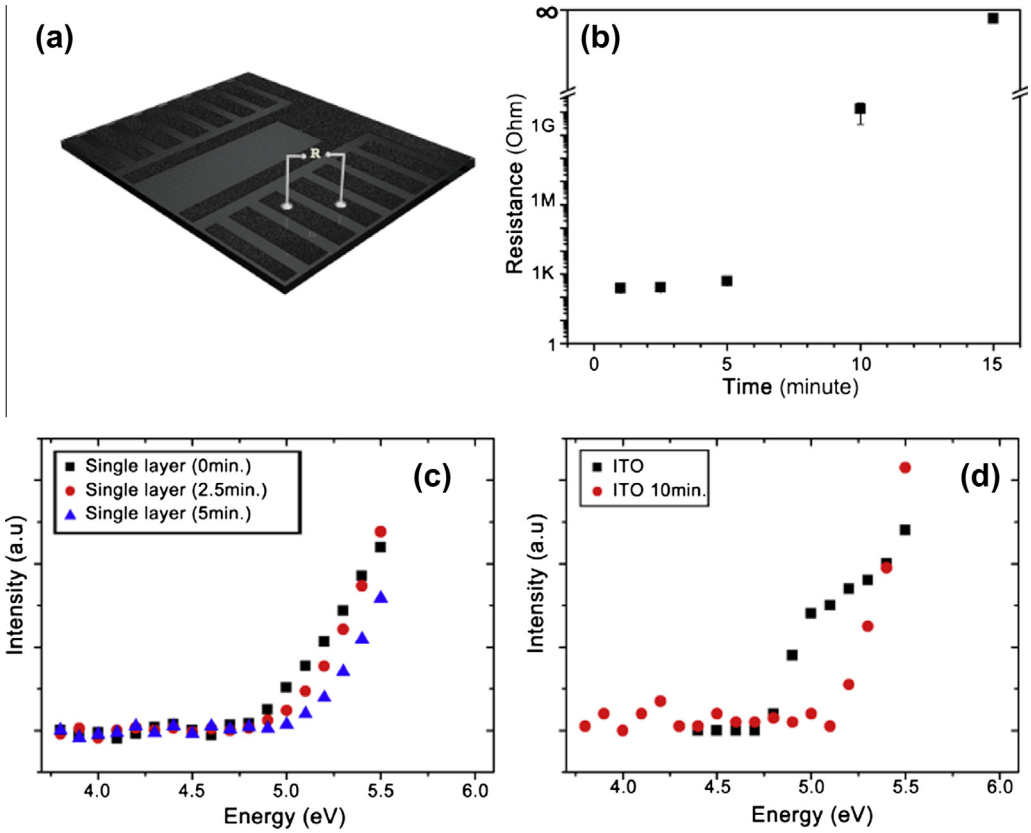

Fig. 3. Patterning and work function of graphene film (a) schematic image of measuring the resistance between adjacent electrodes, (b) resistance between adjacent electrodes, (c) work function of single-layer of graphene following UVO treatment time and (d) work function of ITO following UVO treatment time.

Table 2
The intensity ratio (I_{2D}/I_G) and FWHM of Raman spectra.

	I_{2D}/I_G	FWHM (cm^{-1})
Before UVO treatment	4.521	25.92
After UVO treatment for 1 min	2.768	39.76
After UVO treatment for 2.5 min	2.709	39.78
After UVO treatment for 5 min	1.616	46.72

The results show that the specific contact resistivity of Al is higher than that of Ag, due to poor adhesion of Al, which is consistent with the previous report [28]. The higher contact resistance of Al comes from the delamination of the metal on the graphene films. The cross sectional SEM images showed that Ag has a good adhesion property, but in case of Al, we can see hollow area between Al and graphene film (Fig. 5). This defect causes the higher contact resistance in the contact between Al and graphene. Therefore, we selected Ag as the contact and pad metal materials to fabricate PLEDs with the single-layer graphene anodes.

We measured the current (I) – voltage (V) – luminance (L) characteristic of PLEDs with ITO anode ("ITO PLEDs") and single-layer graphene anode ("graphene PLEDs"). The measured results are shown in our previous report [14]. The turn-on voltages of PLEDs are 3.2 V and 3.6 V for ITO and graphene anodes, respectively. The turn-on voltage is defined at the luminance of 1 cd/m^2. The graphene PLEDs have current level comparable to the ITO PLEDs for biases under 5 V. At bias >5 V, the current level of the graphene PLEDs is lower than that of the ITO PLEDs. The overall light intensity of the graphene PLEDs is lower than the value of the ITO PLEDs due to the high resistivity of the graphene films. The sheet resistance of ITO used in this paper is 10.10 ± 0.11 (Ω/sq) measured by four point probe methods. Fig. 6a shows the external quantum efficiency (EQE) – voltage (V) characteristic of PLEDs. These graphs are the similar to the trend of their light intensity. The maximum external quantum efficiency, current efficiency and power efficiency of the graphene PLEDs are 3.37% (at 1008 cd/m^2, Fig. 6b), 9.73 cd/A (at 761 cd/m^2) and 5.51 lm/W (at 353 cd/m^2), respectively [14]. At 1008 cd/m^2, the efficiencies are 3.37%, 9.59 cd/A, and 4.72 lm/W. For ITO PLEDs, the maximum efficiencies are 4.16% (at 1070 cd/m^2, Fig. 6b) 12.48 cd/A (at 1444 cd/m^2) and 8.01 lm/W (at 125 cd/m^2), respectively [14]. At 963 cd/m^2, the efficiencies are 4.15%, 12.46 cd/A and 7.01 lm/W. The emission photographs of these two devices operating at 0.5 mA appear in inset of Fig. 6b. Fig. 6c shows the spectrum of both PLEDs, which is almost same to each other. The maximum peaks are located at 507 and 509 nm for graphene and ITO PLEDs, respectively. The second peaks are located at 533 and 531 nm for graphene and ITO PLEDs, respectively.

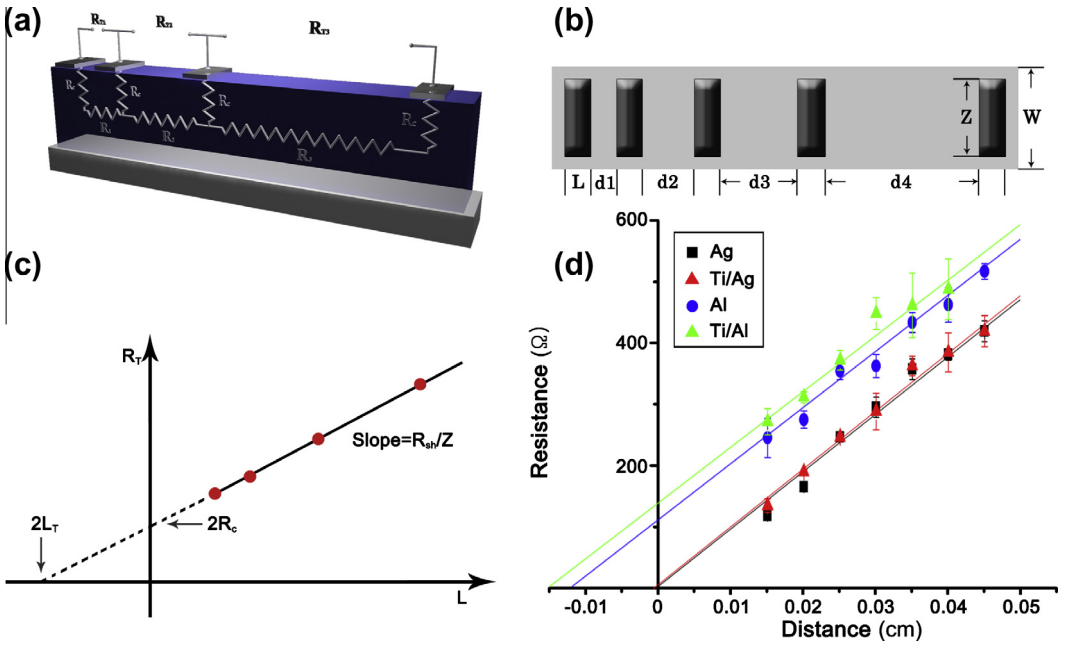

Fig. 4. Transfer length method (TLM) (a) schematic image of TLM, (b) top view of TLM, (c) concept graph of TLM and (d) total resistance between graphene film and metal such as Ag, Al, Ti/Ag, and Ti/Al.

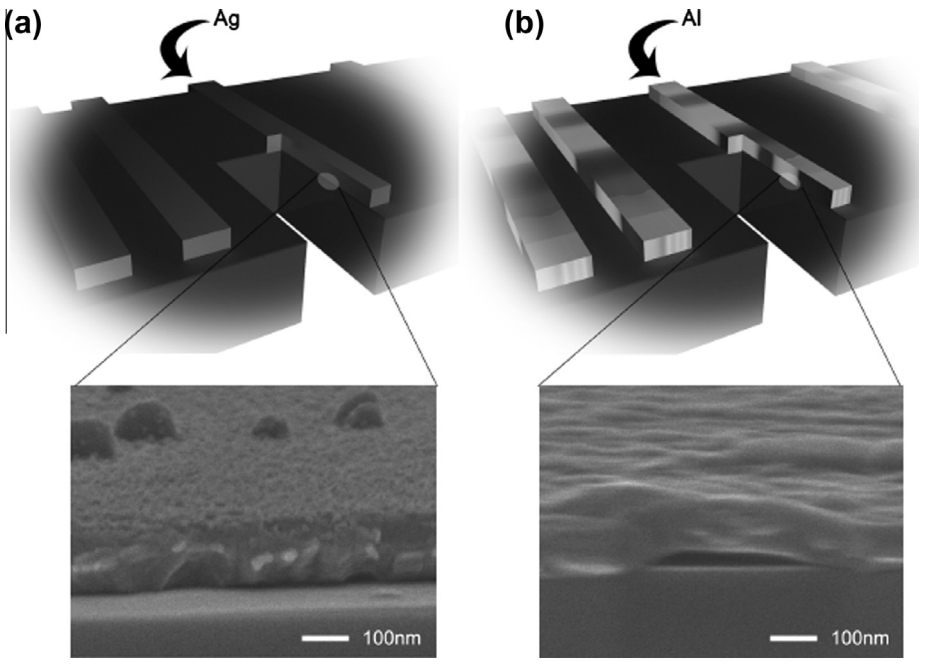

Fig. 5. (a) Schematic image and cross sectional SEM image of Ag/graphene/glass and (b) schematic image and cross sectional SEM image of Al/graphene/glass.

The graphene PLEDs showed comparable performances to ITO PLEDs when the UVO treatment and Ag pads were applied. We suppose that high sheet resistance effect on the degradation of the device performance is more significant for the devices with the large light-emitting area, while it is negligible for the smaller area devices in hundreds of micrometer order such as AMOLED pixels. If additional methods such as chemical doping or hybridization with metal grids are applied simultaneously, the PLEDs performance is expected to be further improved. In addition, it should be noticed that the graphene PLED is free from the Indium diffusion problems between PEDOT:PSS and ITO, which often degrades the device performance.

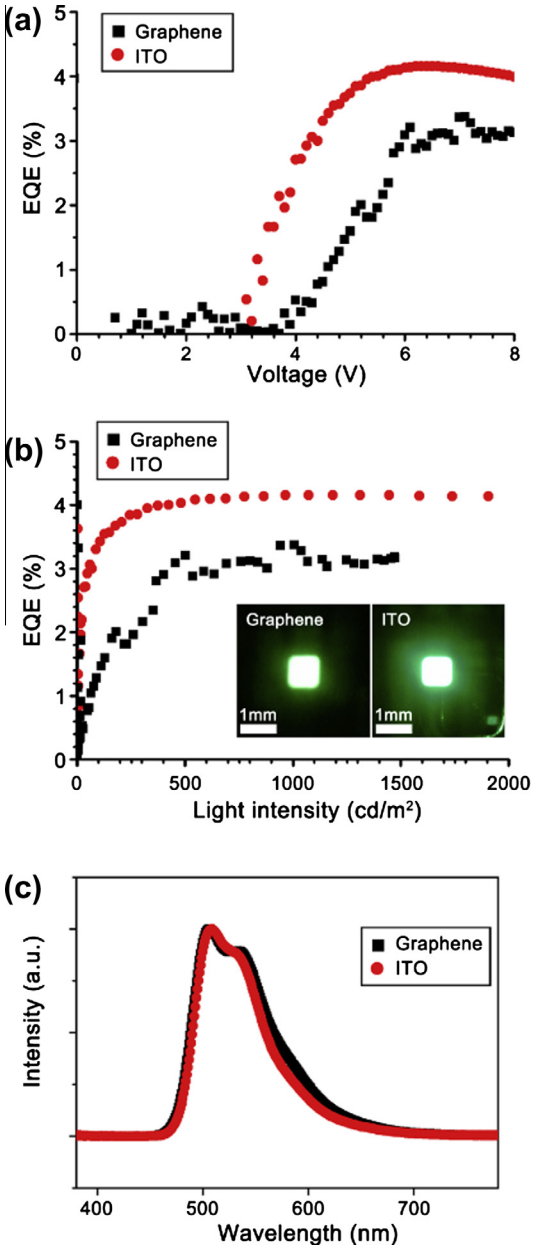

Fig. 6. Electrical properties of the PLEDs (a) external quantum efficiency of PLEDs vs. voltage (EQE-V), (b) external quantum efficiency of PLEDs vs. light intensity (EQE-cd/m^2). The inset figures show the emission image of PLEDs and (c) emission spectrums of PLEDs.

4. Conclusions

In this study, we demonstrated that the single-layer graphene film can be used as the transparent conductive anode of PLEDs. The UVO-assisted patterning and work function engineering are very useful to enhance the performance of PLED devices. Furthermore, the good contact property graphene with our printable Ag electrodes [29] would enable more practical applications to flexible and potentially stretchable displays.

Acknowledgments

This work was supported by the OLED center of Samsung Display and Seoul National University, the Industrial Strategic Technology Development Program (KI002104, Development of Fundamental Technologies for Flexible Combined-Function Organic Electronic Device), the Global Research Lab (GRL) Program (2011-0021972), the Global Frontier Research Program (2011-0031627), and the Basic Science Research Program (2012M3A7B4049807, 2011-0017587 and 2009-0083540) through the National Research Foundation of Korea (NRF) funded by the Korean government (MEST and MKE).

References

[1] K.S. Novoselov, A.K. Geim, S.V. Morozov, D. Jiang, Y. Zhang, S.V. Dubonos, I.V. Grigorieva, A.A. Firsov, Science 306 (2004) 666.
[2] F. Bonaccorso, Z. Sun, T. Hasan, A.C. Ferrari, Nat. Photonics 4 (2010) 611.
[3] J. Wu, M. Agrawal, H.A. Becerril, Z. Bao, Z. Liu, Y. Chen, P. Peumans, ACS Nano 4 (2010) 43.
[4] T. Sun, Z.L. Wang, Z.J. Shi, G.Z. Ran, W.J. Xu, Z.Y. Wang, Y.Z. Li, L. Dai, G.G. Qin, Appl. Phys. Lett. 96 (2010) 133301.
[5] T.-H. Han, Y. Lee, M.-R. Choi, S.-H. Woo, S.-H. Bae, B.H. Hong, J.-H. Ahn, T.-W. Lee, Nat. Photonics 6 (2012) 105.
[6] J. Hwang, H.K. Choi, J. Moon, T.Y. Kim, J.-W. Shin, Appl. Phys. Lett. 100 (2012) 133304.
[7] L.G.D. Arco, Y. Zhang, C.W. Schlenker, K. Ryu, M.E. Thomson, C. Zhou, ACS Nano 4 (2010) 2865.
[8] P. Matyba, H. Yamaguchi, G. Eda, M. Chhowalla, L. Edman, N.D. Robinson, ACS Nano 4 (2010) 637.
[9] P. Matyba, H. Yamaguchi, M. Chhowalla, N.D. Robinson, L. Edman, ACS Nano 5 (2011) 574.
[10] S. Bae, H. Kim, Y. Lee, X. Xu, J.-S. Park, Y.Zheng.J. Balakrishnan, T. Lei, H.R. Kim, Y.I. Song, Y.-J. Kim, K.S. Kim, B. Özyilmaz, J.-H. Ahn, B.H. Hong, S. Iijima, Nat. Nanotechnol. 5 (2010) 574.
[11] C. Brabec, V. Dyakonov, U. Scherf, In Organic Photovoltaics, Wiley-VCH, Weinheim, 2008. pp. 251.
[12] T.W. Lee, M.G. Kim, S.Y. Kim, S.H. Park, O. Kwon, T. Noh, T.S. Oh, Appl. Phys. Lett. 89 (2006) 123505.
[13] Y. Hong, J. Kanichi, IEEE Trans. Electron Devices 51 (2004) 1562.
[14] J. Ha, S. Park, D. Kim, J. Ryu, C. Lee, B.H. Hong, Y. Hong, Proc. SPIE (2012) 84760Y.
[15] K.S. Kim, Y. Zhao, H. Jang, S.Y. Lee, J.M. Kim, K.S. Kim, J.-H. Ahn, P. Kim, J.-Y. Choi, B.H. Hong, Nature 457 (2009) 706.
[16] L. Zhang, S. Diao, Y. Nie, K. Yan, N. Liu, B. Dai, Q. Xie, A. Reina, J. Kong, Z. Liu, J. Am. Chem. Soc. 133 (2011) 2706.
[17] L. Tapasztó, G. Dobrik, P. Lambin, L.P. Biró, Nat. Nanotechnol. 3 (2008) 397–401.
[18] L.C. Campos, V.R. Manfrinato, J.D. Sanchez-Yamagishi, J. Kong, P. Jarillo-Herrero, Nano Lett. 9 (2009) 2600.
[19] N. Severin, S. Kirstein, I.M. Sokolov, J.P. Rabe, Nano Lett. 9 (2009) 457–461.
[20] J. Bai, X. Duan, Y. Huang, Nano Lett. 9 (2009) 2083.
[21] S. Huh, J. Park, Y.S. Kim, K.S. Kim, B.H. Hong, J.-M. Nam, ACS Nano 5 (2011) 9799–9806.
[22] Y. Shi, K.K. Kim, A. Reina, M. Hofmann, L.-J. Li, J. Kong, ACS Nano 4 (2010) 2689–2694.
[23] Y. Yi, W.M. Choi, Y.H. Kim, J.W. Kim, S.J. Kang, Appl. Phys. Lett. 98 (2011) 013505.
[24] Y.-J. Yu, Y. Zhao, S. Ryu, L.E. Brus, K.S. Kim, P. Kim, Nano Lett. 9 (2009) 3430.
[25] W.H. Lee, J. Park, Y. Kim, K.S. Kim, B.H. Hong, K. Cho, Adv. Mater. 23 (2011) 3460–3464.
[26] D.K. Schroder, In Semiconductor Material and Device Characterization, third ed., Wiley-Interscience, New Jersey, 2006.
[27] L.K. Mak, C.M. Rogers, D.C. Northrop, J. Phys. E: Sci. Instrum. 22 (1989) 317.
[28] J.A. Robinson, M. LaBella, M. Zhu, M. Hollander, R. Kasarda, Z. Hughes, K. Trumbull, R. Cavalero, D. Snyder, Appl. Phys. Lett. 98 (2011) 053103.
[29] S. Chung, J. Lee, H. Song, S. Kim, J. Jeong, Y. Hong, Appl. Phys. Lett. 98 (2011) 153110.